Biochemical and Biophysical Research Communications 460 (2015) 589–595

Contents lists available at ScienceDirect

Biochemical and Biophysical Research Communications

journal homepage: www.elsevier.com/locate/ybbrc

Microvesicles released constitutively from prostate cancer cells differ biochemically and functionally to stimulated microvesicles released through sublytic C5b-9

Dan Stratton [a], Colin Moore [a], Samuel Antwi-Baffour [a, 1], Sigrun Lange [b], Jameel Inal [a, *]

[a] Cellular and Molecular Immunology Research Centre, London Metropolitan University, UK
[b] University College London School of Pharmacy, London UK

ARTICLE INFO

Article history:
Received 27 February 2015
Available online 24 March 2015

Keywords:
Constitutive microvesicles
Stimulated microvesicles
Complement inhibition

ABSTRACT

We have classified microvesicles into two subtypes: larger MVs released upon stimulation of prostate cancer cells, sMVs, and smaller cMVs, released constitutively. cMVs are released as part of cell metabolism and sMVs, released at 10-fold higher levels, produced upon activation, including sublytic C5b-9. From electron microscopy, nanosight tracking analysis, dynamic light scattering and flow cytometry, cMVs (194–210 nm in diameter) are smaller than sMVs (333–385 nm). Furthermore, using a Quartz Crystal Microbalance measuring changes in resonant frequency (Δf) that equate to mass deposited on a sensor, an sMV and a cMV are estimated at 0.267 and 0.241 pg, respectively. sMVs carry more calcium and protein, express higher levels of lipid rafts, GPI-anchored CD55 and phosphatidylserine including deposited C5b-9 compared to cMVs. This may allude to biological differences such as increased bound C4BP on sMVs inhibiting complement more effectively.

© 2015 Elsevier Inc. All rights reserved.

1. Introduction

Microvesicle formation results from cell stimulation (activation) or apoptosis. Activation may encompass different stimuli, including chemical, biochemical and mechanical, inducing apoptotic or pseudoapoptotic events (brief exposure to stress initiating an easily recoverable apoptotic event) and/or increases in $[Ca^{2+}]_i$ [1].

Apoptotic events are initiated via cell death signals originating extrinsically such as through FasL or intrinsically by caspase activation and caspase-3 cleavage causing the degradation of cellular protein, including actin. Whereas Membrane Attack Complex (MAC or C5b-9) can induce a caspase-dependent, stimulated apoptosis [2] sublytic levels can be pro- or anti-apoptotic [3].

Besides roles in intercellular communication, MVs are involved in homeostatic mechanisms, ranging from inflammation control to cellular differentiation [4]. Although the physical and biological properties of MVs derived from different cells has been studied, the distinction between constitutively released MVs and those released upon cell stimulation, has not hitherto been attempted.

2. Materials and methods

2.1. Isolation of constitutively released MVs

MVs were isolated as described previously [5]. Exosomes were purified by centrifugation (2 × 100,000 *g*/60 min) after removing MVs. All EVs were quantified and sized by Nanoparticle Tracking Analysis (NTA) using the NanoSight LM20. For comparison, MVs were quantified using the Guava EasyCyte 12HT microcapillary flow cytometer (Millipore), 10,000 events being acquired at a flow rate of 0.6 μl/s. With a resolution down to 0.2 μm, and using a stepper motor pump, the 12HT allows exact volume uptake thus eliminating sheath fluid, enabling absolute particle counts. To avoid counting large debris and MVs, fluorescent or autofluorescent MVs were always gated. When the FSC versus SSC plot was observed with this gate applied, so-called 'backgating,' any debris was thus excluded.

* Corresponding author.
E-mail address: j.inal@londonmet.ac.uk (J. Inal).
[1] Current address: School of Allied Health Sciences, University of Ghana, Accra, Ghana.

http://dx.doi.org/10.1016/j.bbrc.2015.03.074
0006-291X/© 2015 Elsevier Inc. All rights reserved.

2.2. Stimulation of cells with sublytic complement (NHS) or BzATP

This was carried out as described before [5].

2.3. Flow cytometric analysis of C5b-9 deposition

C5b-9 on PC3 cells, presensitized with anti-PC3 serum and incubated with NHS, was detected by fixing the cells in 1% paraformaldehyde (4 °C/15 min). Cells were then washed in PBS and incubated with anti-human C5b-9 neoepitope, clone aE11 (DAKO) (30 min/4 °C) and then goat anti-mouse FITC conjugate and washed. The Median Fluorescence Index (MFI) of bound C5b-9 on cells or MVs was determined by flow cyometry. Cells/MVs stained with secondary antibodies alone served as a control, as did a mouse IgG1.

2.4. Immunodepletion of CD63-positive exosomes

EV-containing culture supernatants were incubated for 18 h/4 °C with biotinylated anti-CD63 (Biolegend) and immune complexes removed using Streptavidin T1 Dynabeads (Life Technologies).

2.5. Dynamic light scattering (DLS) analysis

DLS measurements were performed using a Malvern Zetasizer Nano ZS. Samples of MVs at 1×10^6/ml were diluted 3-fold in EV-free (x2, 0.22 μm filtered; 100,000 *g*/16 h) PBS [5]. Six particle size measurements, were recorded per MV subtype and averages taken.

2.6. Quantification of lipid rafts

Briefly, MVs (1×10^6/ml) in 200 μl cholera toxin subunit B AlexaFluor® 594 (Invitrogen) were incubated (10 min/4 °C). After washing (25,000 *g*/15 min) MVs were added to 200 μl anti-CT-B antibody, incubated (15 min/4 °C) and analysed by flow cytometry. Parent cells were similarly stained for GM_1 ganglioside and analysed by immunofluorescence microscopy.

2.7. Quartz Crystal Microbalance (QCM) analysis

Samples were analysed on the QCM (Q-Sense E1) as described before [6]. Using the Sauerbrey equation, $m = -C\left(\frac{\Delta f}{\nu}\right)$, an estimate of MV mass was possible.

2.8. SDS-PAGE, Western blotting and mass spectrometry

Microvesicles were solubilized in non-reducing sample buffer and electrophoresis and immunoblotting carried out as before [7]. Total protein profiles were visualized by silver or Coomassie staining, the latter for protein identification by mass spectrometry. For this, tryptic digests of in-gel digested excised bands underwent MALDI-TOF/TOF (Bruker) and database searching.

2.9. Complement lysis of T. cruzi metacyclic trypomastigote forms

Metacyclic trypomastigotes were incubated in 50% NHS (37 °C/1 h) with 1.5×10^5 MV/ml and parasite survival quantified using a Neubauer chamber and trypan blue staining, as described before [8].

2.10. Statistical analysis

All readings were obtained in triplicate and experiments repeated 2–3 times. Data are represented as mean ± standard error of the mean. Statistical analysis (unpaired t-test or one-/two-way analysis of variance, ANOVA) was performed using GraphPad Prism software (version 5.0). Significance levels were: $^{*}p < 0.05$, $^{**}p < 0.01$ and $^{***}p < 0.001$.

3. Results

3.1. Sizing of constitutively released MVs (cMVs) and those released upon stimulation (sMVs) using NTA, DLS and sizing beads (flow cytometry)

In isolating PC3 exosomes ($CD63^{high}$, $PtSer^{v.low}$; sucrose density 1.14–1.15 g/ml and 50–90 nm in diameter), as expected, by sucrose gradient, (Fig. 1A and B) we found a second pool of vesicles at 1.04–1.05 g/ml ($CD63^{low}$.$PtSer^{low}$ and ~150–200 nm in diameter). We then collected all constitutively released species of EVs (likely to include exosomes and cMVs) from resting PC3 over a 12 h period. As sizing data obtained using beads cannot be comprehensively related to cells or their EVs [9] NTA was used to size the vesicles. This suggested (Fig. S1A) that some type of MV as well as exosomes had been isolated, (exosomes conventionally ≤100 nm in diameter and MVs ≥100 nm). A small peak at 220 nm (for cMVs) often seen in NTA profiles for exosomes may correspond to the 210 nm cMV NTA peak in Fig. 1C, where separately purified exosomes, sMVs and accumulated cMVs (immunodepleted or not of exosomes) were analysed. This showed a modal sMV peak of 350 nm (49.5% of vesicles within 320–380 nm) and a modal cMV peak of 210 nm (33.3% of vesicles within 180–240 nm); the modal peak for exosomes was 100 nm. Whilst immunodepletion of exosomes reduced the exosome counts by ~70%, whilst leaving cMV yield undepleted (Fig. S1B), and reduced the Alix and CD63 signals (Western blotting) (Fig. S1C), removal of the 15,000 *g* pellet from the 100,000 *g* fraction specifically removed the cMV peak (Fig. S1D).

DLS measurements were also used to verify relative MV sizes (Fig. 1D). Despite a wider range, they confirmed sMVs as larger, averaging just over 300 nm in diameter, cMVs, being ~200 nm.

Sizing beads (Fig. 1E) showed cMVs/sMVs to differ considerably in average size and scatter plot. The cMV population had the highest density of events (80%) in the ≤0.3 μm range. sMVs were more uniformly sized with 60% in the >0.3–0.5 μm range. The shape of the respective scatter density plots also differed, each having a unique signature, sMVs showing a narrower SCC-HLog scatter, as a measure of granularity (intravesicular structural complexity and/or membrane topography) than cMVs. sMVs (from MAC-stimulated cells) showed raised levels of relative granularity compared to cMVs (released from unstimulated cells).

As expected, sMVs were released in larger numbers (2.5×10^5/ml within 30 min) than cMVs, (one order of magnitude greater) from the same number of cells in half the time, in response to stressing agents (Fig. S1E) and after 20 min showed some early apoptosis, albeit only 9% (Fig. S1F).

3.2. Transmission electron microscopy of sMVs, cMVs and exosomes

Transmission electron microscopy (TEM) [6] highlighted differences in EV morphology and size. In Fig. 2A, cMVs are small, roughly spherical vesicles (averaging 194 ± 42 nm across, n = 143). sMVs are larger (average diameter 385 ± 55 nm, n = 201) Summarising the data in Fig. 2B collating cMV/sMV sizes by TEM, NTA, DLS and sizing beads, cMVs are 194–210 nm and sMVs 333–385 nm in diameter.

3.3. Mass determination of MVs using the QCM

Using the QCM, we found sMVs to quench the oscillating momentum of the crystal more rapidly than cMVs, implying faster deposition on the sensor and larger mass (Fig. 2C). Given a Δf of

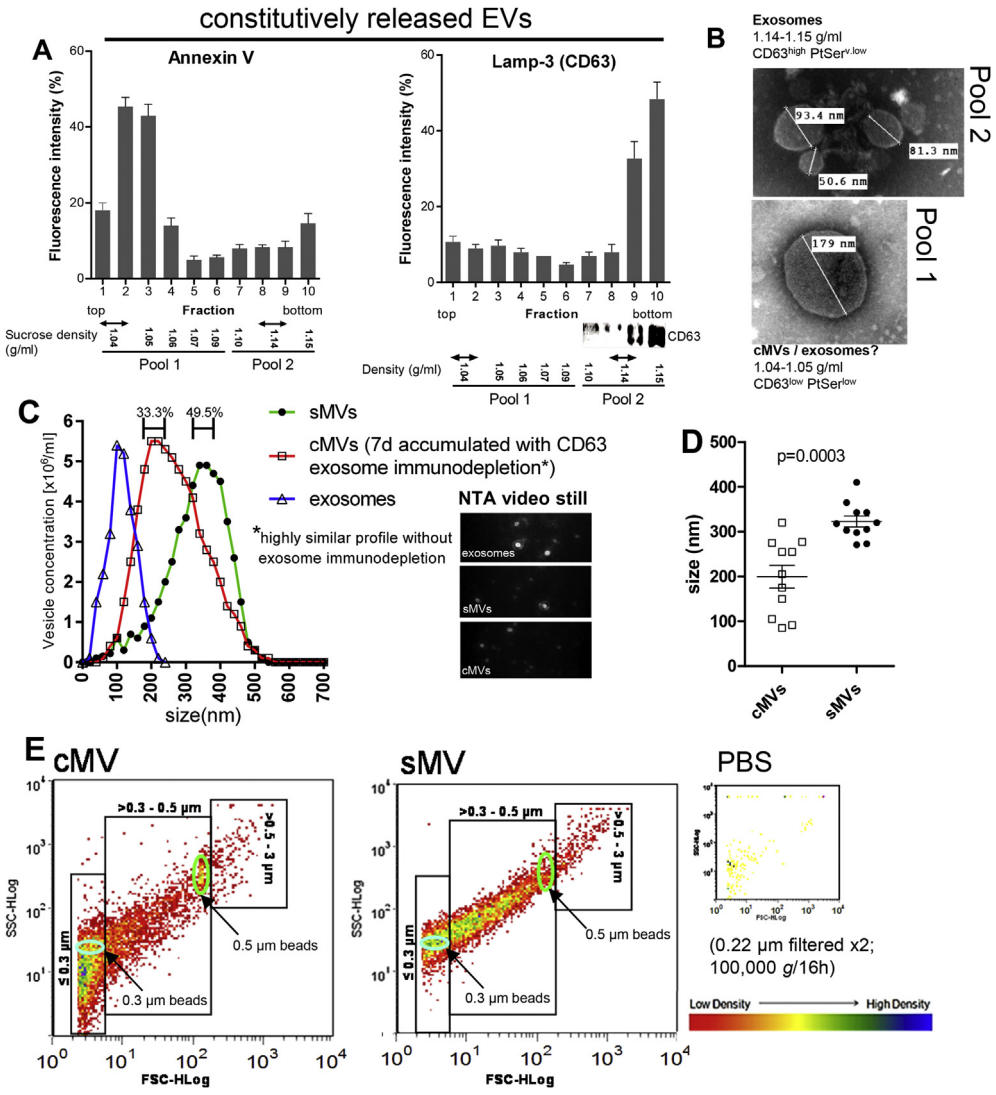

Fig. 1. Constitutively released MVs (cMVs) are larger than those released upon stimulation (sMVs). Pool 1 being AnV-positive, CD63-negative and pool 2 AnV-negative, CD63-positive (A) consisting of vesicles of >100 nm (B) respectively constitute MVs and exosomes. (C) MVs were isolated from PC3 cells, presensitized with anti-PC3 serum and stimulated with 5% NHS (for sMVs) or from the culture supernatants of unstimulated cells (for cMVs) which were (or not) further immunodepleted for CD63-positive exosomes as were exosomes by differential centrifugation; sizes were determined by NTA. A representative screen shot image from the light scatter video shows optimal light scatter (inset). (D) Light scattering by DLS shows sMVs averaging at 333 ± 12 nm and cMVs at 199 ± 25 nm. (E) cMVs and sMVs showed differing population densities by flow cytometry, according to forward (FSC-Hlog) and side scatter (SSC-Hlog). sMV scatter plots show a more uniform distribution of vesicles, most being in the >0.3–0.5 µm range, cMVs being ≤0.3 µm. The FACS gating shown is based upon multimix sizing beads, the oval in the ≤0.3 µm gating representing the 0.3 µm diameter beads and that in the >0.3–0.5 µm gating representing 0.5 µm beads. The data shown is from a single, representative experiment.

300 ± 10 Hz for the deposition of 1.3×10^6 sMVs and 271 ± 7 Hz for the same number of cMVs, sMV and cMV mass was estimated at 0.267 ± 0.008 and 0.241 ± 0.006 pg respectively ($p < 0.05$), the latter agreeing remarkably well with the 0.25 pg, calculated earlier from the mass shed from stimulated cells [6]. An equivalent drop of water (assuming a sphere and 356 nm diameter as for sMVs), would be 0.19 pg, very close to the MV average, 0.259 pg (Fig. 2D).

3.4. Sublytic C5b-9 deposited on cells is effectively removed on sMVs

To confirm MV capacity to remove sublytic C5b-9 from cells, complexes deposited and remaining on PC3 cells were estimated. The highest MFI for C5b-9 was at time zero, straight after 10 min deposition (Fig. 3A). Over 45 min the relative amount of C5b-9 (MFI) reduced from 80.6 to 31.3, and the estimated half-life of C5b-9 decay was 25 min (Fig. 3A, inset). This $t_{1/2}$ is less than that found for C5b-9 removal from K562 cells ($t_{1/2}$ = 38 min) [10] but more comparable with the vesiculation shown in Fig. S1F (over in 20–30 min); the other factor, not considered here for C5b-9 removal, is endocytosis [10].

sMVs carrying significant C5b-9 (Fig. 3B), raises the possibility of intercellular transfer. Higher C5b-9 levels on sMVs than cMVs, could explain the higher proportion of sMVs in the range >0.3–0.5 µm, having increased granularity, as found in Fig. 1E; similarly, increased deposition of mannose binding lectin (MBL) on apoptotic, as opposed to healthy cells was also perceived as an increase in side scatter [2].

3.5. sMVs expose more PtSer, have higher levels of deposited C4BP and carry more protein but have fewer lipid rafts than cMVs

Both MV populations were confirmed as MVs, as opposed to exosomes, through labelling with AnV-FITC (Fig. 3C). The bimodal

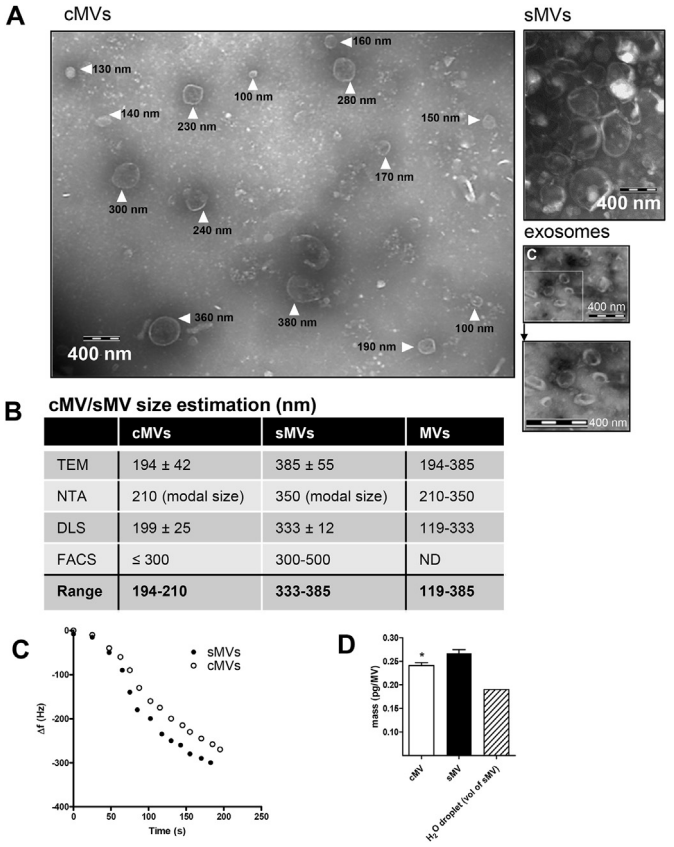

	cMVs	sMVs	MVs
TEM	194 ± 42	385 ± 55	194-385
NTA	210 (modal size)	350 (modal size)	210-350
DLS	199 ± 25	333 ± 12	119-333
FACS	≤ 300	300-500	ND
Range	**194-210**	**333-385**	**119-385**

Fig. 2. Transmission electron microscopy of sMVs, cMVs and exosomes. All EVs in (A), were released from PC3 cells. Samples were prepared by negative staining and examined on a JEOL JEM-1200 EXII electron microscope. (B) Average sizes were estimated from several images, 385 ± 55 nm for sMVs, n = 201, and 194 ± 42 nm for cMVs, n = 143. These were compared with those obtained previously by NTA, DLS and by sizing beads. (C) The QCM used at a crystal oscillation of 70 MHz to measure the ability of MVs to quench oscillating momentum showed sMVs to phase out quicker indicating faster deposition, and larger mass; estimated masses calculated using the Sauerbrey equation are shown in D.

histogram for PtdSer exposition on sMVs revealed PtSer low and high populations, the latter likely representing remnant cMVs, binding AnV less strongly; this asymmetric sMV peak also makes comparisons of fluorescent intensities difficult although comparing the 'PtSer High' sMV peak with the unimodal cMV 'PtSer' peak would suggest higher exposition on sMVs. This is reminiscent of scatter plots for unstimulated monocytes releasing MVs (which we would now term 'cMVs') showing lower granularity compared to 'sMVs' released from calcium ionophore-treated cells [11]. Those 'sMVs' also showed a bimodal distribution for the AnV histogram and a unimodal one for 'cMVs' [10].

The soluble complement inhibitor, C4BP (C4b-binding protein), complexed to protein S in serum, bound MVs (Fig. 3D). This was mediated through binding surface PtdSer as preincubation with AnV blocked the interaction. The binding of complexed C4BP via exposed PtdSer (and protein S), on apoptotic cells, has been described before [12]. That the binding was greater on sMVs (Fig. 3D), presumably reflects their greater PtSer exposition.

As expected, given that sublytic C5b-9-stimulated cells are associated with increased DNA synthesis, cell proliferation and *de novo* protein synthesis [13] we found sMVs to contain more protein/MV, 0.035 pg protein/sMV and 0.022 pg protein/cMV (Fig. S2A). However, sMVs with a 5-fold greater volume (based on average diameters determined above) would, per unit volume contain about 1/3rd the amount of protein in cMVs. SDS-PAGE (Fig. S2B) showed a wider profile of protein bands, in the 30–250 kDa range in sMVs. Uniquely it also showed high MW proteins, likely components of deposited C5b-9, (bracketed and highlighted with an asterisk) and was more akin to the protein profile of unstimulated cells whose profile in turn appeared to have several proteins that are diminished in cells after sMV release (lane with C5b-9-stimulated cells) as denoted by white triangles (Fig. S2B).

Although there are few proteins (marked †) present in the resting (unstimulated) parent cells greatly diminished/absent in sMVs/cMVs, overall we cannot intimate any particular protein sorting from these profiles, which constitute a preliminary analysis. So far, mass spectrometry (Fig. S2C) and Western blotting (Fig. S2D) has confirmed abundant proteins (annexin VI, pyruvate kinase, α-tubulin, β-actin) in sMVs.

Decay Accelerating Factor (DAF) is GPI-anchored, enriched on lipid rafts (sphingolipid- and cholesterol-rich areas) [14] and likely to be enriched on MVs. DAF on MVs, was more highly expressed than on parent cells (iMFI 369 for sMVs and 210 for cMVs compared to 154 for parent cells) (Fig. S2E and F) as a reflection of the comparatively high expression of lipid rafts on sMVs. In Fig. S2F we show integrated mean MFI (iMFI) as the product of the relative frequency of cells or MVs (percent positive) and MFI for GM_1 ganglioside expression (as a measure of lipid rafts). Thus, as well as acquiring greater levels of C4BP, sMVs express more DAF with possible implications in complement inhibition.

3.6. sMVs inhibit complement-mediated lysis more effectively than cMVs

Having previously shown host cell MVs to interact with and inhibit complement-mediated lysis of *Trypanosoma cruzi* [8] we found sMVs to more effectively protect *T. cruzi* parasites from complement-mediated lysis (Fig. S3).

4. Discussion

Microvesicles may be categorised, according to their mode of generation, and certain physical and biochemical properties, into two groups. Working with prostate cancer cells we have distinguished MVs, into constitutively released, cMVs, and stimulated, sMVs (Fig. 4). In a recent study on human myeloma cells, size distribution of MVs released upon stimulation, this time by serum deprivation (SD), was also increased in a similar size range, [15]. In early SD, where tumour cells, unlike their normal counterparts, have anti-apoptotic responses initiated, there was a 1.5-fold increase in % of 'stimulated' MVs in the 0.2–0.5 μm range in two myeloma cells lines [15]; in this study we found a 3.8-fold increase in % PC3 sMVs versus cMVs in the >0.3–0.5 μm range. This is in contrast to previous work on THP-1 cells where the stimulus, including LPS, had no effect on size distribution of MVs compared to those released without stimulus. In this case there were proportionally low numbers, ~30% of the total of MVs in the <190 nm, 190–530 nm and 530–780 nm ranges combined compared to the 780–990 nm (~60%) probably because of the relatively low centrifugation speed used during isolation (16,000 *g*/45 min). Our estimated sizes using sizing beads and TEM, were confirmed by DLS, with sMVs and cMVs in the range 333–385 nm and 194–210 nm, respectively. Despite the inherent deficiencies in all size determination methods [16], the trend of larger sMVs (from C5b-9-stimulated cells) than cMVs, was consistent.

Whereas 'extrinsic' apoptosis is triggered by death ligand–receptor interaction and the perforin pathway by cytotoxic T cells (and perforin), cells also undergo constitutive, spontaneous apoptosis. This occurs via the intrinsic pathway and may be part of normal, low level, continuous cell turnover and homeostasis,

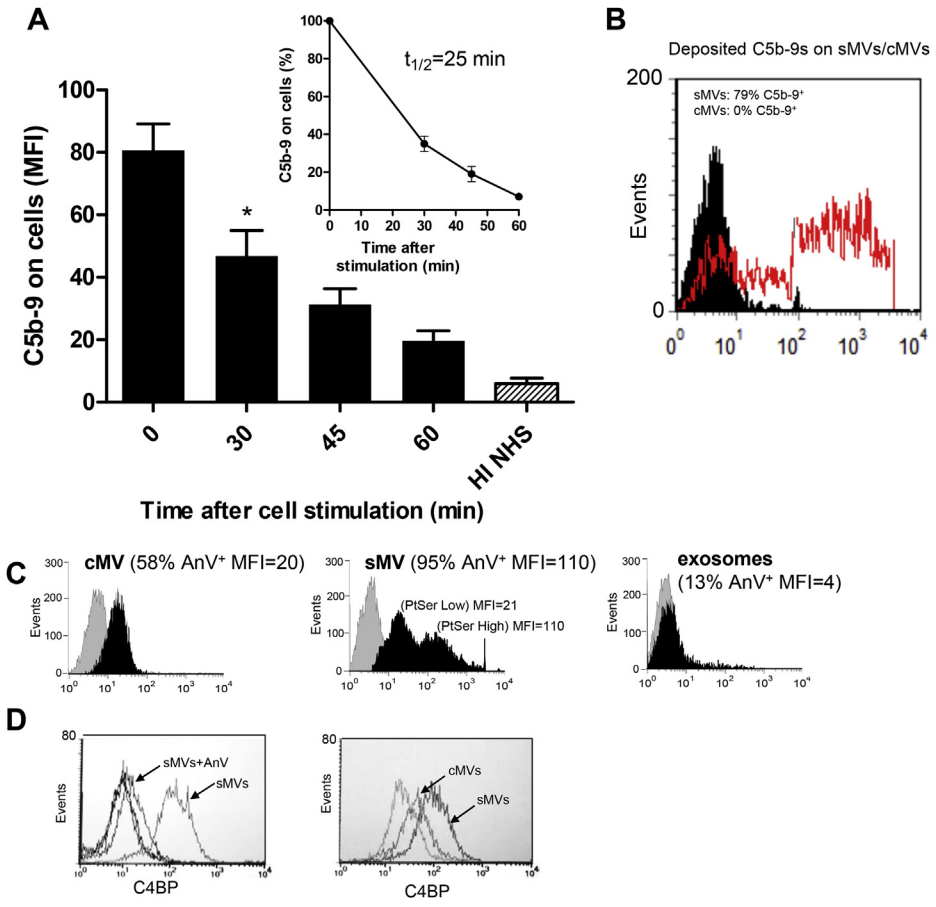

Fig. 3. Decay curve for loss of deposited C5b-9 from cells coincides with high levels of C5b-9 on sMVs. Presensitized PC3 cells were treated with sublytic doses of C5b-9 (5% NHS) for 30, 45 and 60 min at 37 °C (A). At these times the cells were washed and labelled with anti-human C5b-9 (clone aE11), a FITC-labelled secondary antibody and analysed by FACs (MFI) whilst considering control fluorescence from cells labelled without primary antibody. The data were represented as percentage expression of deposited C5b-9, inset, to give an estimate of the half-life of C5b-9 decay. (B) Cells stressed with sublytic complement release MVs harbouring higher levels of bound C5b-9 than cMVs. (C) % AnV-FITC binding as a measure of PtdSer expression on cMVs (58%) compared to sMVs (95%) and exosomes (13%). (D) sMVs incubated in NHS (20%) (~40 μg/ml C4BP) at 37 °C/30 min had bound C4BP detected with sheep anti-human C4BP and FITC-conjugated anti-sheep IgG. The binding was abrogated by preincubation for 30 min/RT with 50 nM annexin V. In the second panel C4BP binding is greatest on sMVs.

triggered by negative signals such as deprivation of cytokines, growth factors or hormones (so-called starvation-induced apoptosis) that de-represses death programmes. This occurs in normal cell culture leading to the release of cMVs (Fig. 4A). The intrinsic pathway may also be triggered by positive signals, hypoxia, free radicals, virus infection, toxins, heat and radiation [17] leading to sMV release. Another positive signal, sublytic C5b-9 deposition, results in Ca^{2+} influx, mitochondrial overload and loss of mitochondrial transmembrane potential ($\Delta\Psi_m$) leading to cytochrome *c*-mediated activation of caspase and apoptosis [18].

sMVs are released in response to stress factors, probably as a mechanism to circumvent apoptosis [19]. Most mammalian cells exist in a state of pseudoapoptosis, an apoptotic-like state from which they can readily revert [1]. If left to accrue, stress factors ultimately result in apoptosis or even necrosis [18]. The uncontrolled rise in $[Ca^{2+}]_i$ from membrane pores such as MAC (Fig. 4B) but also from intracellular stores such as ER [20] could lead to metabolic damage, but also act as second messengers for many intracellular signalling pathways [10].

MV release, if a cellular response to injury may contribute to the 'shedding' of excess intracellular calcium, helping restore basal levels between 7 and 15 min after cell stimulation, akin to the export of damaging agents such as deposited C5b-9 and caspase-3, allowing the cell to recover.

The higher PtSer exposition on MVs (and from other studies also in apoptotic blebs) is likely due to the different mechanisms of biogenesis, exosomes having an endocytic origin and MVs, certainly sMVs, being associated with early apoptosis. In addition we found sMVs to have higher intravesicular calcium, express more PtSer, to be larger and carry more protein (Fig. 4A and B). sMVs carry more lipid rafts and GPI-anchored CD55 (DAF) likely sequestered to lipid rafts, was as expected more highly expressed in sMVs. That annexin VI, the phospholipid-binding protein involved in exocytosis and endocytosis, detected in MVs, is an equally strong band in cMVs and sMVs, unlike the other proteins, suggests a particular lack of incorporation in sMVs. This may relate to the rapid (within 5s) cytosolic calcium-mediated translocation of annexin VI to the plasma membrane, observed in THP-1 and other cells, in this case calcium ionophore-mediated [21]; plasma membrane-located Annexin VI for some reason may then not so readily be incorporated into sMVs.

The QCM was able to provide an accurate measure of sMV and cMV mass (0.267 and 0.241 pg, respectively) which agreed with previous calculations based on loss in mass of stimulated cells [6].

Previously we showed host MVs, to interact with and protect *Trypanosoma cruzi* from complement-mediated lysis, and from *in vivo* experiments to enable the parasite to infect host cells [8]. We now show cMVs to offer less protection against complement lysis

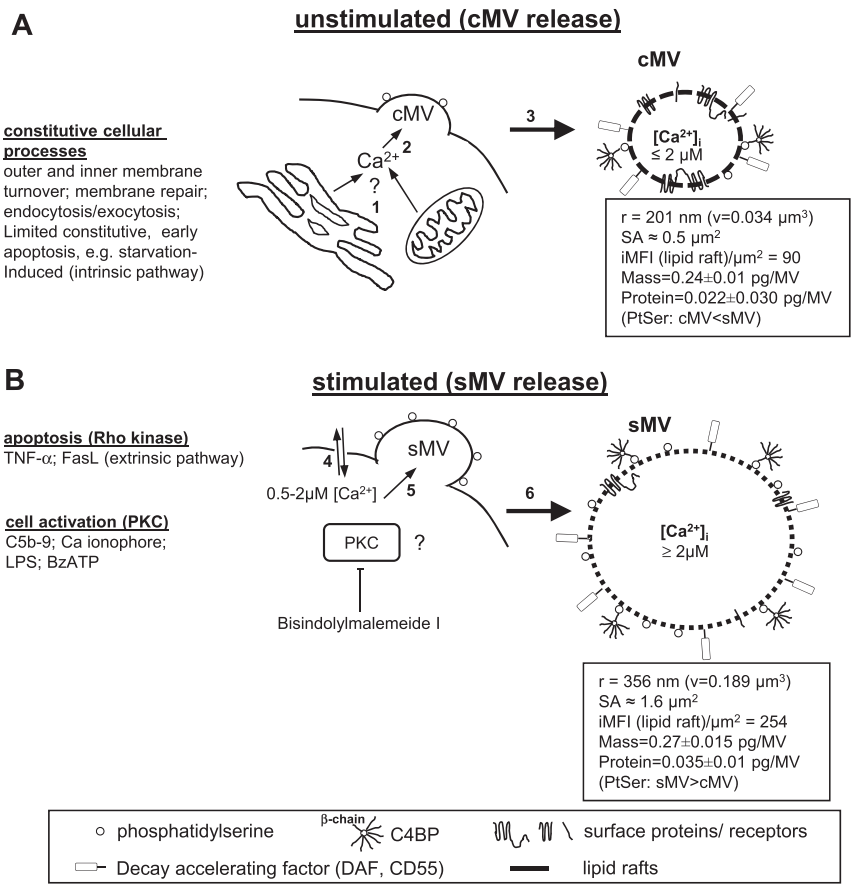

Fig. 4. Model for formation and properties of MV subtypes. cMVs are released from cells during normal metabolism (A): **1**, Calcium is released from organelles causing calpain-mediated actin cleavage and membrane depolarisation leading to formation of a pro-cMV bleb. **2**, The bleb may be formed by protein and lipid sorting leading to distinctive cMV characteristics, **3**. sMVs are released as a result of cell stress or injury (B): **4**, Higher concentrations of extracellular calcium enter the cell via sublytic MAC or an activated calcium channel/membrane breach. The organelles are unable to sequester the influxed calcium. **5**, free calcium causes actin cleavage and membrane depolarisation in an uncontrolled manner leading to rapidly produced bleb, **6**. sMVs bleb and pinch off. This may be abrogated by blocking protein kinase C [5]. Per MV, larger sMVs have higher overall protein levels, more DAF (GPI-anchored protein), lipid rafts, PtSer and associated C4BP, than cMVs.

than sMVs, perhaps the smaller cMVs having a lesser avidity for complement deposition; this may be important if MVs are simply depleting complement. Increased C4BP on sMVs may also play a role. Besides being a co-factor for factor I-mediated cleavage of C3b/C4b [22], C4BP binds and inactivates C3 convertase [23]. Although DAF is more expressed in sMVs, these types of comparisons are difficult with different sized MVs and need further confirmation.

There has been much speculation in the EV field about heterogeneity of MV and exosome sizes, including in MVs from activated platelets, of differences in protein content, according to size class and associated differences in function [24]. The immunodepletion of exosomes suggests that differential centrifugation may not be ideal to separate them from cMVs, but shows the populations are distinct. Also cMV size (and lack of laddered DNA) means they are devoid of apoptotic blebs which would certainly be released from a few cells dying in culture. sMVs are primarily released through apoptotic triggers, including sublytic MAC, BzATP and calcium ionophore and may possibly transmit such apoptotic signals. Furthermore, the increased PtSer on sMVs, carrying stress agents, may facilitate their more rapid phagocytosis. This may be significant in autoimmune disease as we previously showed MVs to inhibit apoptotic cell phagocytosis [25] possibly explaining decreased phagocytic activity in atherosclerotic plaques [26]. Conversely, the smaller, low PtSer-positive cMVs, may be less phagocytosed and pass unhindered through the tissues to perform their communicative role.

Conflict of interest

The authors declare that there are no conflicts of interest.

Acknowledgments

This work was part funded by the Sir Richard Stapely Educational Trust (to S. A-B.) and HEFCE QR funding (RAE2008).

Appendix A. Supplementary data

Supplementary data related to this article can be found at http://dx.doi.org/10.1016/j.bbrc.2015.03.074.

Transparency document

Transparency document related to this article can be found online at http://dx.doi.org/10.1016/j.bbrc.2015.03.074.

References

[1] A.B. Mackenzie, M.T. Young, E. Adinolfi, et al., Pseudoapoptosis induced by brief activation of ATP-gated P2X7 Receptors, J. Biol. Chem. 280 (2005) 33968–33976.
[2] A.J. Nauta, M.R. Daha, O. Tijsma, et al., The membrane attack complex of complement induces caspase activation and apoptosis, Eur. J. Immunol. 32 (2002) 783–792.

[3] O. Bohana-Kashtan, L. Ziporen, N. Donin, et al., Cell signals transduced by complement, Mol. Immunol. 41 (2004) 583–597.
[4] J.M. Inal, E.A. Ansa-Addo, D. Stratton, et al., Microvesicles in health and disease, Arch. Immunol. Ther. Exp. 60 (2012) 107–121.
[5] D. Stratton, C. Moore, L. Zheng, S. Lange, J.M. Inal, Prostate cancer cells stimulated by calcium-mediated activation of protein kinase C undergo a refractory period before re-releasing calcium-bearing microvesicles, Biochem. Biophys. Res. Commun. (2015), http://dx.doi.org/10.1016/j.bbrc.2015.03.061.
[6] D. Stratton, S. Lange, J.M. Inal, Label-free real-time acoustic sensing of microvesicle release from prostate cancer (PC3) cells using a Quartz Crystal Microbalance, Biochem. Biophys. Res. Commun. 453 (2014) 619–624.
[7] K.M. Hui, G.L. Orriss, T. Schirmer, et al., Expression of functional recombinant von Willebrand factor-A domain from human complement C2: a potential binding site for C4 and CRIT, Biochem. J. 389 (2005) 863–868.
[8] I. Cestari, E. Ansa-Addo, P. Deolindo, et al., *Trypanosoma cruzi* immune evasion mediated by host cell-derived microvesicles, J. Immunol. 188 (2012) 1942–1952.
[9] R. Lacroix, S. Robert, P. Poncelet, et al., Standardization of platelet-derived microparticle enumeration by flow cytometry with calibrated beads: results of the International Society on Thrombosis and Haemostasis SSC Collaborative workshop, J. Thromb. Haemost. 8 (2010) 2571–2574.
[10] O. Moskovich, Z. Fishelson, Live cell imaging of outward and inward vesiculation induced by the complement C5b-9 complex, J. Biol. Chem. 282 (2007) 29977–29986.
[11] N. Satta, F. Toti, O. Feugeas, et al., Monocyte vesiculation is a possible mechanism for dissemination of membrane-associated procoagulant activities and adhesion molecules after stimulation by lipopolysaccharide, J. Immunol. 153 (1994) 3245–3255.
[12] J.H. Webb, A.M. Blom, B. Dahlbäck, The binding of protein S and the protein S-C4BP complex to neutrophils is apoptosis dependent, Blood Coagul. Fibrinolysis 14 (2003) 355–359.
[13] L.R. Benzaquen, A. Nicholson-Weller, J.A. Halperin, Terminal complement proteins C5b-9 release basic fibroblast growth factor and platelet derived growth factor from endothelial cells, J. Exp. Med. 179 (1994) 985–992.
[14] D. Lingwood, K. Simons, Lipid rafts as a membrane-organizing principle, Science 327 (2010) 46–50.
[15] L. Sun, H.-X. Wang, X.-J. Zhu, et al., Serum deprivation elevates the levels of microvesicles with different size distributions and selectively enriched proteins in human myeloma cells *in vitro*, Acta Pharmacol. Sin. 35 (2014) 381–393.
[16] Z. Varga, Y. Yuana, A.E. Grootemaat, et al., Toward traceable size determination of extracellular vesicles, J. Extracell. Vesicles 3 (2014), http://dx.doi.org/10.3402/jev.v3.23298.
[17] S. Elmore, Apoptosis: a review of programmed cell death, Toxicol. Pathol. 35 (2007) 495–516.
[18] K. Triantafilou, T.R. Hughes, M. Triantafilou, et al., The complement membrane attack complex triggers intracellular Ca^{2+} fluxes leading to NLRP3 inflammasome activation, J. Cell. Sci. 126 (2013) 2903–2913.
[19] M.N. Abid Hussein, A.N. Boing, A. Sturk, et al., Inhibition of microparticle release triggers endothelial cell apoptosis and detachment, Thromb. Haemost. 98 (2007) 1096–1107.
[20] R. Rizzuto, T. Pozzan, Microdomains of intracellular Ca^{2+}: molecular determinants and functional consequences, Physiol. Rev. 86 (2006) 369–408.
[21] M.G. Pittis, R.C. Garcia, Annexins VII and XI are present in a human macrophage-like cell line. Differential translocation on FcR-mediated phagocytosis, J. Leukoc. Biol. 66 (1999) 845–850.
[22] A.M. Blom, B.O. Villoutreix, B. Dahlbäck, Mutations in alpha-chain of C4BP that selectively affect its factor I cofactor function, J. Biol. Chem. 278 (2003) 43437–43442.
[23] I. Gigli, T. Fujita, V. Nussenzweig, Modulation of the classical pathway C3 convertase by plasma proteins C4 binding protein and C3b inactivator, Proc. Natl. Acad. Sci. U. S. A. 76 (1979) 6596–6600.
[24] W.L. Dean, M.J. Lee, T.D. Cummins, et al., Proteomic and functional characterisation of platelet microparticle size classes, Thromb. Haemost. 102 (2009) 711–718.
[25] S. Antwi-Baffour, S. Kholia, Y.K.-D. Aryee, et al., Human plasma membrane-derived vesicles inhibit the phagocytosis of apoptotic cells – possible role in SLE, Biochem. Biophys. Res. Commun. 396 (2010) 278–283.
[26] P.-E. Rautou, A.-C. Vion, N. Amabile, et al., Microparticles, vascular function, and atherothrombosis, Circ. Res. 109 (2011) 593–606.